PHYSICAL REVIEW B, VOLUME 65, 125205

Free-carrier dynamics in low-temperature-grown GaAs at high excitation densities investigated by time-domain terahertz spectroscopy

Gregor Segschneider, Frank Jacob, Torsten Löffler, and Hartmut G. Roskos
Physikalisches Institut, Johann Wolfgang Goethe-Universität, Robert-Mayer-Straße 2-4, D-60054 Frankfurt am Main, Germany

Sönke Tautz, Peter Kiesel, and Gottfried Döhler
Institut für Technische Physik I, Friedrich Alexander-Universität, Erwin-Rommel-Straße 1, D-91058 Erlangen, Germany
(Received 12 April 2001; revised manuscript received 31 May 2001; published 12 March 2002)

We investigate the dynamics of the high-frequency conductivity of optically excited low-temperature-grown GaAs (LT-GaAs)—a material widely used for photoconductive switching in ultrafast optoelectronics—by time-resolved terahertz (THz) transmission spectroscopy. This contactless technique is insensitive to the nonlinear interband response of the material which complicates the analysis of all-optical pump/probe measurements. For material grown and annealed at or near temperatures, which are optimal for photoconductive switching, we find a slowing down of the decay of the conductivity (respectively, the carrier density) with rising excitation density. We associate the increase of the decay time with a saturation of the available trap states whose density is estimated to be on the order of $2\times10^{18}\,\mathrm{cm}^{-3}$.

DOI: 10.1103/PhysRevB.65.125205 PACS number(s): 72.20.Jv, 72.20.Ee, 72.80.Ey

LT-GaAs grown by molecular beam epitaxy at low temperatures (growth temperature T_g: 210–230 °C) under arsenic overpressure and subsequently annealed at $T_a \approx 600\,^\circ\mathrm{C}$ has found many applications in ultrafast optoelectronic switching and as electrical insulator in microelectronics.[1] The reason is the very high electrical resistivity and the extremely short lifetime of the charge carriers in this material. Both properties result from the unique composition of the material. During the growth process, many point defects like neutral and positively charged arsenic antisites ($\mathrm{As}^0_{\mathrm{Ga}}$,$\mathrm{As}^+_{\mathrm{Ga}}$) are incorporated. Their density depends strongly on both T_g and T_a. While the combined density right after the growth is on the order of $10^{20}\,\mathrm{cm}^{-3}$, it decreases during the annealing process to values from $5\times10^{17}\,\mathrm{cm}^{-3}$ to $5\times10^{18}\,\mathrm{cm}^{-3}$.[2–4] At the same time, the excess arsenic coalesces and forms crystalline precipitates which have diameters of several nanometer and a density on the order of $10^{18}\,\mathrm{cm}^{-3}$.[5] The charged antisites as well as the arsenic precipitates are believed to play important roles with respect to the electrical and optoelectronic properties of the material but at present neither the exact mechanisms nor the relative contribution of the two kinds of defects are understood.[6,7]

Charge carriers, either injected electrically or generated optically, have a high mobility as long as they are in the conduction respectively valence band. The mobility decays rapidly, however, because of ultrafast relaxation of the carriers into trap states below the mobility edges. The trap states may be either Urbach tail states resulting from the disorder in the material and energetically located right below the band edges of pure GaAs, or midgap states associated with the defects and arsenic clusters. It is a favorable feature of LT-GaAs that all trap states are sufficiently deep that thermal reactivation of carriers, once they are trapped, is insignificant for all practical purposes. As long as the carriers remain in the trap states, they may still participate in the screening of electrical fields. The electrical influence is terminated only when electrons and holes recombine.

The time scales of these processes were studied in the past by time-resolved optical experiments. Reflectivity measurements with both the pump and the probe photon energies being well above the bandgap of GaAs yielded effective trapping-time constants τ_1 as low as 200 fs.[8] It is doubtful, however, whether the data were interpreted correctly, because such measurements are likely to probe rather the dynamics of electrons within the conduction band than the carrier trapping process. More reliable are data obtained by experiments where the probe photon energy is chosen to be close to the bandgap of GaAs. Such measurements yielded values of τ_1 of 300–500 fs.[9] Carriers may be trapped either in Urbach tail states or in midgap states. Those trapped in Urbach tail states undergo further relaxation into deeper states on a time scale of >1 ps. This is known from two-color all-optical pump/probe measurements with the probe energy being located slightly below the bandgap of GaAs.[10] The final relaxation by carrier recombination can be traced by two-color experiments which probe trap states at photon energies several hundred meV below the bandgap.[9,11] Values for the effective recombination time τ_2 of 10 ps are reported.

It is a practical concern in ultrafast optoelectronics whether saturation of trap states may lead to a degradation of the performance of LT-GaAs-based photoconductive switches at high excitation densities. Although some evidence exists for a saturation-induced reduction of both the bandwidth and the efficiency of the generation respectively detection of THz signals,[12] the knowledge about saturation in LT-GaAs is surprisingly limited. In the past, only the group of Whitaker investigated saturation in a somewhat systematic way.[13,14] A slowing down of carrier trapping with increasing density was reported. In addition, measurements at a fixed high excitation density were performed by Benjamin *et al.*[15] A study by Siegner *et al.* was restricted to as-grown (unannealed) material.[16] All of these experiments were all-optical transmission measurements which have the common drawback that it is difficult to extract detailed information from these measurements because nonlinear optical phenomena

 ©2002 The American Physical Society

such as the Auger effect, bandgap renormalization, two-photon absorption processes, reexcitation of untrapped and trapped carriers, and ionization of normally neutral defect states complicate the analysis in the strong-excitation regime.

The data analysis is less complex for probe energies in the midinfrared or farinfrared spectral range where only intraband transitions are relevant, which means that only free carriers contribute to a change of the signal. For that reason, we study trap-state saturation with time-resolved terahertz (THz) probing, a method well established for the determination of frequency-dependent conductivities[17] and applied already in the past for studies of carrier dynamics in LT-GaAs in the low-excitation limit.[18]

We investigate a series of LT-GaAs films grown by molecular beam epitaxy at temperatures of $T_g=210$, 235, 245, and 275 °C, respectively. All samples are annealed at $T_a=600$ °C. Another sample, grown at 275 °C is annealed at 700 °C. The sample thickness is 0.5 μm for the sample grown at 210 °C and 1.0 μm for all others. Pieces of the wafers are attached to sapphire platelets either by wafer bonding (the sample grown at 210 °C) or with UV-curing epoxy (all other samples). The GaAs substrate is then removed by wet-chemical etching in order to avoid charge carriers photogenerated in the substrate to contribute to the signal in the time-resolved experiments.

During the measurements, the samples are mounted on a copper plate with a pin-hole of 2.5 mm diameter acting as effective aperture. The measurements are performed with the samples held at room temperature.

The experimental setup is described in Ref. 19. Optical pulses of 150 fs duration and photon energies of 1.57 eV are provided by a Clark 2001 laser system running at a repetition rate of 1 kHz. The beam is split into three parts. The first one (the pump beam) excites charge carriers in the LT-GaAs sample; the beam diameter on the sample is 3.5 mm, larger than the aperture, in order to guarantee a laterally homogeneous excitation. The beam is chopped at half the laser repetition rate thus providing the modulation necessary for lock-in detection. The second beam generates THz probe pulses in a large-aperture GaAs antenna. The probe pulses transmitted through the LT-GaAs sample are then detected by mixing them with the third pulse (detection pulse) in an electrooptically active ZnTe crystal with a thickness of 1 mm.[20] The time delay between the probe pulse and the detection pulse is fixed at a position where the amplitude of the probe pulse is maximal, while the time delay between the pump pulse and the probe pulse is varied. The temporal resolution of our measurements is approximately 350 fs as can be deduced from the rise time of the signals displayed in Fig. 2.

In Fig. 1, we demonstrate the capabilities of the technique with data for the sample annealed at 700 °C, well above the optimal temperature. In this case, the signal decay is slow because of the reduced trap density, and both the trapping and the recombination of the carriers occur with exponential time dependences as will be shown later. The main panel of Fig. 1 displays the pump-induced change of the transmitted THz amplitude for four different excitation densities. Three of the curves are shifted along the time axis for reasons to be explained later. At the lowest excitation density (initial electron-hole pair density) of $1.5\times10^{16}\,\mathrm{cm}^{-3}$, the signal decays exponentially. This is not the case, however, at elevated densities where the relative transmission change becomes quite large and may even approach unity. At the highest excitation density of $9\times10^{17}\,\mathrm{cm}^{-3}$ in Fig. 1, the relative transmission change amounts to 0.48 where signal saturation is already quite significant.

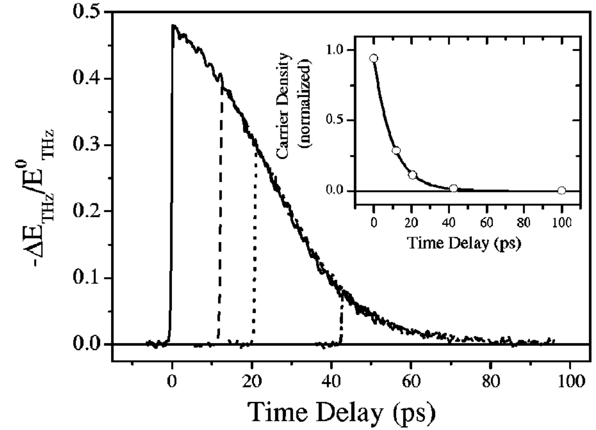

FIG. 1. Main panel: Time dependence of the THz differential transmission signal for the sample annealed at 700 °C for excitation densities of $1.5\times10^{16}\,\mathrm{cm}^{-3}$, $1.1\times10^{17}\,\mathrm{cm}^{-3}$, $3.3\times10^{17}\,\mathrm{cm}^{-3}$, and $9\times10^{17}\,\mathrm{cm}^{-3}$, respectively. E^0_{THz} is the transmitted THz amplitude without optical pumping. The lower-density curves are shifted in time to overlap with the curve for the highest density. Inset: Carrier density versus time shift and exponential fit to the data with a time constant of 9.5 ps.

This does not imply, however, a nonexponential carrier dynamics but only demonstrates the extremely high sensitivity of the THz signal to highly mobile free carriers. If the signals of Fig. 1 are shifted horizontally, they can be positioned such that they overlap perfectly with each other (this is the way how the data are actually displayed in Fig. 1). Obviously, the signal depends only on the density of the untrapped carriers at any given moment which is only possible, if the relaxation dynamics is not affected by trap filling. The exponential decay characteristics of the free-carrier population is extracted in the following way. In the inset of Fig. 1, we plot the excitation densities of five measurements (four of them displayed in the main panel) versus the temporal shifts needed to overlap the curves. We then fit an exponential curve to the data points which indeed are found to lie perfectly on top of the fit curve. The decay time constant, i.e., the carrier trapping time, is $\tau_1=9.5$ ps. This value is in good agreement with the trapping time of 9 ps obtained by us by an all-optical pump/probe measurement with the pump and probe photon energies being identical and chosen to be near the bandgap of GaAs.

Sample heating by the optical excitation apparently does not affect our measurements in a significant way. Thermal effects reveal themselves by the formation of a barely discernible long-lived pedestal in the trailing part of the signal resulting from the refractive index change of the sample.

We now turn to the four samples annealed at 600 °C and investigate the carrier dynamics from low excitation densi-

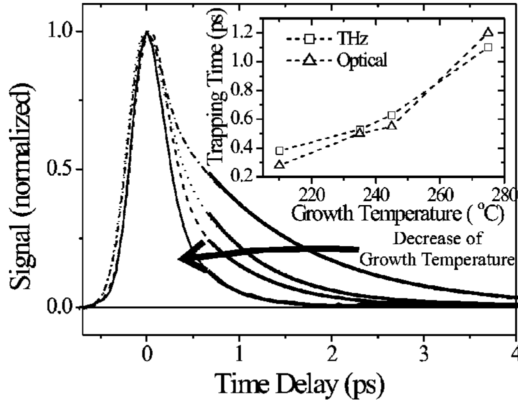

FIG. 2. Low-excitation THz differential transmission curves for all samples annealed at 600 °C. The relative changes of the THz-pulse amplitude at time delay zero are 0.35 ($T_g = 210\,°\mathrm{C}$), 0.31 (235 °C), 0.34 (245 °C), and 0.45 (275 °C). Fit curves to the data are also displayed (dark lines). The inset shows the dependence of the trapping time τ_1 on the growth temperature. Data obtained by the fitting procedure are compared with data extracted from all-optical pump/probe experiments.

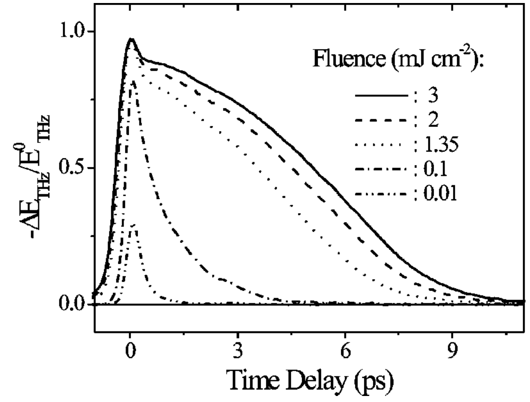

FIG. 3. THz differential transmission signal of the sample grown at 210 °C.

ties up to very high densities. Figure 2 compares the THz transmission change for an excitation density of $5 \times 10^{17}\,\mathrm{cm}^{-3}$, i.e., in the low-excitation regime where trap filling is still negligible. The curves reproduce the well-known fact that τ_1 depends on the growth temperature and is minimal at values of T_g of about 210 °C.[8]

To extract values for τ_1 from the transients, we model the transmission of a THz pulse through the sample with the transfer-matrix method using time-dependent Fresnel coefficients for transmission and reflection. The complex index of refraction of the LT-GaAs layer is calculated from the Drude dielectric function $\epsilon(\omega,t) = \epsilon_{\mathrm{stat}} - \omega_p^2(t)/[\omega(\omega + i\Gamma)]$. Here $\omega_p(t)$ denotes the plasma frequency $\omega_p(t) = \sqrt{N(t)e^2/m^*\epsilon_0}$, with $N(t)$ being the time-dependent density of free (untrapped) charge carriers with reduced effective mass m^*. Γ is the collision rate of the carriers which is assumed to be time independent. The value of the static dielectric constant ϵ_{stat} is set to $\epsilon_{\mathrm{stat}} = 13.1$. The dielectric function and the conductivity $\sigma(\omega,t)$ are connected by the relation $\epsilon(\omega,t) = \epsilon_{\mathrm{stat}} + i\sigma(\omega,t)/(\omega\epsilon_0)$. We neglect plasmon-phonon coupling[21] after having verified that it modifies the overall transmission change of the electromagnetic field in our frequency range by less than 2%. This is well below the uncertainty of the determination of the field amplitude in the experiment.

In the low-excitation limit, where the density of trap states exceeds the density of photogenerated charge carriers, the carrier population decays exponentially: $\omega_p^2 \propto N_0 \exp(-t/\tau_1)$. With this knowledge, and by calculating the excitation density from the pump-pulse intensity assuming linear-absorption conditions, one can fit the experimental data with the model by adjusting only two parameters, Γ and τ_1. To avoid complications by the time resolution and by hot-carrier effects, the fits cover only the data obtained at delay times of more than 0.6 ps.

The scattering time defined as Γ^{-1} varies little for the samples grown at 210, 235, and 245 °C and is found to be 15–20 fs. Scattering hence is faster in these LT-GaAs samples than in pure GaAs.[22] For the sample grown at 275 °C, the fit procedure yields a scattering time of 50 fs closer to the situation of pure GaAs. One is led to conclude that scattering at arsenic precipitates and point defects dominates Γ in the case of material grown and annealed close to optimal conditions. A reduction of the defect density by raising T_g reduces the scattering rate.

From the latter, one can estimate the mobility μ of the optically excited free carriers in LT-GaAs with the relation $\mu = e/(\Gamma m^*)$. Assuming the reduced effective mass m^* to be the same as in single-crystalline GaAs, the mobility for growth temperatures at or below $T_g = 245\ °\mathrm{C}$ is calculated to be in the range of 450–550 $\mathrm{cm}^2/(\mathrm{Vs})$. These values lie in the middle of the wide range of mobilities [164–3000 $\mathrm{cm}^2/(\mathrm{Vs})$] reported for LT-GaAs grown under comparable conditions.[2,18,23–25] For the highest of our growth temperature, $T_g = 275\ °\mathrm{C}$, the mobility is enlarged to a value of 1400 $\mathrm{cm}^2/(\mathrm{Vs})$.

The inset of Fig. 2 displays the values obtained for τ_1 as a function of T_g. In addition, it shows values of τ_1 which we determined by single-line pump/probe measurements with photon energies of 30 meV above the GaAs bandgap. The values are in very good agreement with each other. The dependence on T_g matches that reported in Ref. 8. It is noteworthy that the signal decay time measured in our THz-probing experiments does not correspond at all to the longer time constant measured in Ref. 10 which was associated with the relaxation of charge carriers from Urbach tail states into deeper trap states. This implies that electrons once they are in the Urbach tail states are reduced in mobility to such a high degree that they do not contribute to a THz transmission change anymore. In the terminology of the potential-fluctuation picture (Anderson localization model) one can say that the mobility edges of the investigated samples must be located very close to the energy band edges of pure GaAs.

We now investigate the high-excitation-density regime. Figure 3 shows a set of transient THz signals for the sample grown at 210 °C and pumped at fluences from 0.01 $\mathrm{mJ\,cm}^{-2}$ up to 3 $\mathrm{mJ\,cm}^{-2}$. Assuming linear-absorption conditions, the excitation density is estimated to be $1.5 \times 10^{20}\,\mathrm{cm}^{-3}$ at the

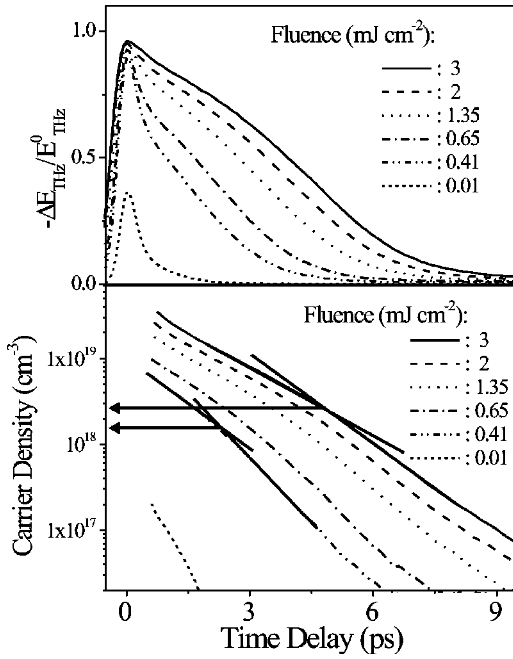

FIG. 4. Upper panel: THz differential transmission signal of the sample grown at 235 °C. Lower panel: Time dependence of the free-carrier density of the same sample as extracted from the Drude model.

highest fluence and $5\times10^{17}\,\mathrm{cm}^{-3}$ at the lowest one. Except for the latter, the excitation density is always larger than the densities of both the available $\mathrm{As}^{+}_{\mathrm{Ga}}$ antisites and the arsenic clusters. For the four high-excitation curves, the relative transmission change at time delay zero (positioned arbitrarily at the maximal signal) is close to unity. The decay dynamics varies with the excitation density and it is not possible anymore to overlap the curves by shifting them temporally as in Fig. 1. This is clear evidence for the occurrence of trap saturation. The decay of the signal is not determined by the carrier trapping process anymore but rather by trap emptying whose dynamics we assume to be closely associated with that of carrier recombination.

The upper panel of Fig. 4 displays a corresponding set of transient THz signals for the sample grown at the slightly higher temperature of 235 °C. The pump fluences (nominal excitation densities) range from 0.01 $\mathrm{mJ\,cm}^{-2}$ ($4.5\times10^{17}\,\mathrm{cm}^{-3}$) up to 3 $\mathrm{mJ\,cm}^{-2}$ ($1.4\times10^{20}\,\mathrm{cm}^{-3}$). The data of Fig. 4 are very similar to those of Fig. 3, all the main feature are reproduced and even the time scales do not differ significantly. Again, trap saturation makes it impossible to overlay the curves with each other by temporal shifting.

The lower panel of Fig. 4 depicts the time dependence of the carrier density obtained from the data of the upper panel by their evaluation with the Drude dielectric function under the assumption of a fixed scattering time constant Γ^{-1} of 15 fs. The data begin at a delay time of 0.7 ps because hot-carrier effects and the limited time resolution prevent the fit procedure to reproduce the experimental data at earlier times. At the lowest excitation density, the carrier density decays exponentially with a time constant of 0.55 ps. This value corresponds to the carrier trapping time constant τ_1 of 0.5 ps derived from the data of Fig. 2 for this sample.

The decay becomes slower and non-exponential when the excitation density is raised. The temporal evolution of the carrier density is then characterized by a kink in the curves separating a slower initial relaxation from a faster decay at later times. For the highest excitation density and the second lowest density the kinks are highlighted by straight lines approximating the curves above and below the kinks. The increase of the decay rate may result from the end of saturation, when the relaxation is again dominated by carrier trapping instead of trap emptying. It is interesting to note that the kink occurs at carrier densities on the order of $2\times10^{18}\,\mathrm{cm}^{-3}$, a value which corresponds to the density of $\mathrm{As}^{+}_{\mathrm{Ga}}$ defects expected for our material. This agreement may be evidence for a significant role of $\mathrm{As}^{+}_{\mathrm{Ga}}$ antisites in the carrier recombination process.

The decay dynamics remains difficult to understand in spite of the separability of the decay into a sequence of two quasiexponential segments. First, it remains unclear why the decay at later delay times (after the kink) remains slower than the carrier trapping time in the weak-excitation limit represented by the data for a pump fluence of 0.01 $\mathrm{mJ\,cm}^{-2}$. It appears that a sizeable density of trap states remains occupied and hence unavailable for trapping of other free carriers. Carrier trapping would then be slowed down. Secondly, the overall decay of the carrier density is distinctly faster than expected from Refs. 9, 11 which report trap emptying times τ_2 in the range of 10 ps for LT-GaAs grown and annealed at similar temperatures as our material. However, these experiments explored only the regime of low excitation densities. Apparently, trap emptying is faster at the high excitation densities of our experiments. One can only speculate about the underlying mechanism. Processes which depend on the momentary carrier density, e.g., a density-dependent recombination time, appear feasible. Another possibility is an excitation-dependent increase of the density of recombination centers. One could imagine that defects such as the $\mathrm{As}^{0}_{\mathrm{Ga}}$ defect which normally are electrically neutral and inactive are ionized and activated as recombination centers either by the pump pulse directly or by subsequent scattering processes.

We finally investigate the sample grown at 275 °C. The upper panel of Fig. 5 presents the relative THz transmission change and the lower panel the calculated carrier density as a function of delay time. Qualitatively, the features of the data are very similar to those of the samples grown at lower values of T_g, except that the time scale is expanded by a factor of approximately 2. The relaxation of the carrier population is slowed down because of the reduced densities of defects and arsenic clusters, an observation which supplements a similar one for the low-excitation regime as discussed in conjunction with Fig. 2. The dynamics close to delay time zero differs from that of the other two samples discussed before. At the highest excitation densities, the signal at time delay zero does not increase with rising pump power any more. The reason is unknown at present. The small bump at a delay time of 12.5 ps results from a reexcitation of the sample by a weak reflected optical beam.

The dynamics of the carrier density is obtained from the

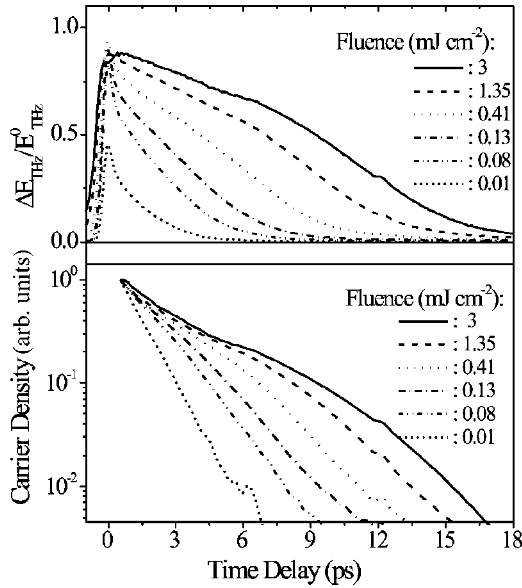

FIG. 5. Upper panel: THz differential transmission signal of the sample grown at 275 °C. Lower panel: Time dependence of the free-carrier density of the same sample as extracted from the Drude model. Here, the carrier densities are normalized for easier comparison of the decay dynamics.

data by fitting under the assumption of a time-independent scattering time constant Γ^{-1} of 50 fs. Figure 6 depicts the initial carrier density obtained in this way as a function of the nominal value calculated under the approximation of linear absorption. Above $2\times10^{19}\,\mathrm{cm}^{-3}$, the nominal and the actual densities differ from each other corroborating the expectation that the relative pump absorption decreases with pump fluence in the high-excitation regime.

We turn again to the temporal evolution of the carrier density in the lower panel of Fig. 5. For the lowest pump fluence, the carrier density exhibits a single-exponential decay behavior with a time constants of 1.1 ps which agrees well with the trapping time constant for this sample in Fig. 2. For higher fluences, a kink develops as in the data for the

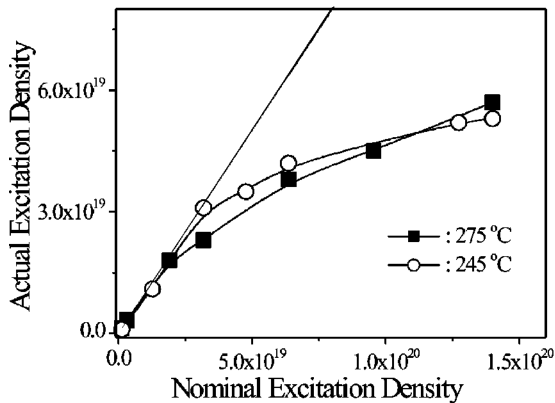

FIG. 6. Comparison of the free-carrier density extrapolated to zero time delay with the nominal carrier density for the samples grown at 245 and at 275 °C. The straight line shows the case of linear absorption.

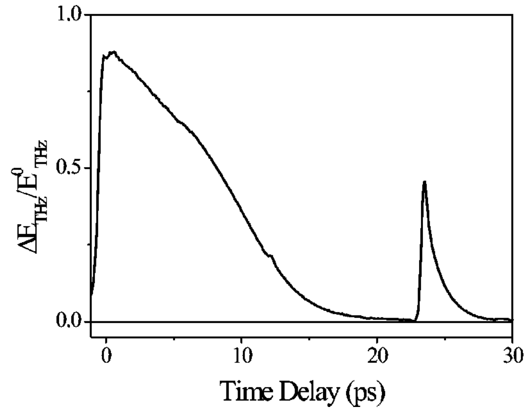

FIG. 7. THz differential transmission signal of the sample grown at 275 °C with fluence of 2 mJ cm^{-2} over a time window of 30 ps showing a weak reexcitation.

two samples grown at lower T_g but in an even more pronounced way. In addition, we find at very high pump fluences and during the first 6 ps that the decay is rather fast at first before it slows down (and becomes faster again at the kink discussed before). We interpret the very rapid early decay and the subsequent slowing down as an artifact of the assumption of a constant scattering rate Γ. Although a density-dependent and hence time-dependent Γ is more realistic we did not take this into account in our fit procedures because the exact dependence of Γ on the density is unknown. Assuming a rise of Γ with time can lead to such a change of the calculated carrier density that the rapid decay at small delay times becomes less pronounced or even vanishes. In fact, an increase of the value of Γ with time is physically plausible. At the extremely high excitation densities of our experiments, screening of Coulomb interactions should be quite efficient, the material should behave metal-like.[26] With decreasing carrier density, screening becomes less efficient. Hence scattering of the charge carriers with defects and clusters (the dominant scattering process in our samples as shown above) should become more significant and with it the value of Γ should increase as argued above.

One may wonder whether a similar feature (a rapid initial decay followed by a slower one) is present in the data of Fig. 4. If it appears at the same carrier densities as in Fig. 5, however, then it should occur at very early delay times <0.7 ps which is not displayed in the lower panel of Fig. 4 because an analysis of the raw data with our simple model is made impossible in this time window by hot-carrier effects and the limited time resolution.

We now turn again to the relaxation of the charge carriers at the highest excitation densities and explore once more the late delay times beyond the kink. Here, the decrease of the carrier density is faster than right before the kink, but slower than the decay observed at low-excitation densities. We argued above (Fig. 4) that this observation may be explained by a continued blockage of some trap states which remain unavailable for trapping of other free carriers for a prolonged period of time. Figure 7 provides evidence that this blockage does not extend for times longer than a few ten ps. Figure 7

shows differential THz transmission data of the sample grown at 275 °C for a pump fluence of 2 mJ cm^{-2}. The data are shown over a longer time window than before. In addition to the signal discussed so far, one observes a second one beginning at a delay time of 23 ps which results from a delayed excitation of the LT-GaAs film by a part of the pump pulse which is reflected twice within the sapphire substrate. The intensity of the second pump pulse amounts to just 1% of the main pulse and hence provides only a weak reexcitation of the sample. The rather high amplitude of the THz transmission signal is again indicative for the high sensitivity of THz probing of free carriers. The important feature is now the decay of the second signal. It occurs monoexponentially with a time constant of 1.2 ps which corresponds closely to the value of 1.2 ps measured for weak excitation of the sample without a prepulse. The trap states apparently have recovered completely within the time scale of 20–25 ps.

We point out that attempts to model the carrier relaxation process with the rate-equation ansatz of Ref. 13 fail at high excitation densities. As discussed above, it is insufficient to describe the relaxation simply by two time constants and to neglect the dependence of major parameters such as Γ, the trapping time τ_1, trap emptying time τ_2, or the trap-state density on the carrier density. The simple model in Ref. 13 leads to the surprising result of a decrease of the trap emtying time τ_2 with rising growth temperature and hence decreasing density of traps. This is counterintuitive because one would expect rather larger values of τ_2 at reduced trap-site densities. In fact, our data are consistent with this expectation.

In summary, we have investigated the dynamics of optically excited free carriers in LT-GaAs by measuring the THz-frequency conductivity of thin films via THz transmission experiments. With rising excitation density, a significant slowing down of the decay of the conductivity, respectively the carrier density, is observed. For all excitation densities of our experiments, however, the conductivity of material grown and annealed at or close to optimal values decays within 10 ps without leaving a long-lived residual conductivity.

[1] M. R. Melloch, J. M. Woodall, E. S. Harmon, N. Otsuka, F. H. Pollak, D. D. Nolte, R. M. Feenstra, and M. A. Lutz, Annu. Rev. Mater. Sci. **25**, 547 (1995).

[2] D. C. Look, D. C. Walters, G. D. Robinson, J. R. Sizelove, M. G. Mier, and C. E. Stutz, J. Appl. Phys. **74**, 306 (1993).

[3] K. F. Pfeiffer, S. Tautz, P. Kiesel, S. Malzer, and G. H. Döhler, Appl. Phys. Lett. **77**, 2349 (2000).

[4] X. Liu, A. Prasad, W. M. Chen, A. Kurpiewski, A. Stoschek, Z. Liliental-Weber, and E. R. Weber, Appl. Phys. Lett. **65**, 3002 (1994).

[5] M. Luysberg, H. Sohn, A. Prasad, P. Specht, Z. Liliental-Weber, E. R. Weber, J. Gebauer, and R. Krause-Rehberg, J. Appl. Phys. **83**, 561 (1998).

[6] A. J. Lochtefeld, M. R. Melloch, J. C. P. Chang, and E. S. Harmon, Appl. Phys. Lett. **69**, 1465 (1996).

[7] H. Ruda and A. Shik, Phys. Rev. B **63**, 085203 (2001).

[8] K. A. McIntosh, K. B. Nichols, S. Verghese, and E. R. Brown, Appl. Phys. Lett. **70**, 354 (1996).

[9] P. Grenier and J. F. Whitaker, Appl. Phys. Lett. **70**, 1998 (1997).

[10] G. Segschneider, T. Dekorsy, R. Hey, and K. Ploog, Appl. Phys. Lett. **71**, 2779 (1997).

[11] T. Dekorsy, G. Segschneider, M. Nagel, H. M. Heiliger, R. Hey, K. Ploog, and M. Luysberg, Symposium on Non-Stoichiometric III-V Compounds, Erlangen **6**, 85 (1998).

[12] H.-M. Heiliger, M. Vossebrger, H. G. Roskos, H. Kurz, R. Hey, and K. Ploog, Appl. Phys. Lett. **69**, 2903 (1996).

[13] T. S. Sosnowski, T. B. Norris, H. H. Wang, P. Grenier, and J. F. Whitaker, Appl. Phys. Lett. **70**, 3245 (1997).

[14] C. Y. Sung, H. H. Wang, T. B. Norris, and J. F. Whitaker, Proc. CLEO, 454 (1996).

[15] S. D. Benjamin, H. S. Loca, and P. W. E. Smith, Appl. Phys. Lett. **68**, 2544 (1996).

[16] U. Siegner, R. Fluck, G. Zhang, and U. Keller, Appl. Phys. Lett. **69**, 2566 (1996).

[17] T. I. Jeon, D. Grischkowsky, A. K. Mukherjee, and R. Meon, Appl. Phys. Lett. **77**, 2452 (2000).

[18] S. S. Prabhu, S. E. Ralph, M. R. Melloch, and E. S. Harmon, Appl. Phys. Lett. **70**, 2419 (1997).

[19] T. Lffler, F. Jacob, and H. G. Roskos, Appl. Phys. Lett. **77**, 453 (2000).

[20] Z. G. Lu, P. Campbell, and X.-C. Zhang, Appl. Phys. Lett. **71**, 593 (1997).

[21] M. V. Klein, in *Light Scattering in Solids* 1 (Springer-Verlag, Berlin, 1988), Vol. 8, p. 147.

[22] F. W. Wise, I. A. Walmsley, and C. L. Tang, Appl. Phys. Lett. **51**, 605 (1987).

[23] N. Zamdmer, Q. Hu, K. A. McIntosh, and S. Verghese, Appl. Phys. Lett. **75**, 2313 (1999).

[24] M. Stellmacher, J.-P. Schnell, D. Adam, and J. Nagle, Appl. Phys. Lett. **74**, 1239 (1999).

[25] H. Němec, A. Pashkin, P. Kužel, M. Khazan, S. Schnüll, and I. Wilke, J. Appl. Phys. **90**, 1303 (2001).

[26] H. Haug, and S. Koch, *Quantum Theory of the Optical and Electronic Properties of Semiconductors* (World Scientific, Singapore, 1990).